

Basal Plane Dislocation Slip Band Characterization and Epitaxial Propagation in 4H SiC

Gil Chung^{1,a*}, Robert Viveros^{1,b}, Charles Lee^{1,c}, Andrey Soukhojak^{1,d},
Vladimir Pushkarev^{1,e}, Qianyu Cheng^{2,f}, Balaji Raghothamachar^{2,g},
Michael Dudley^{2,h}

¹SK siltron css, 1311 Straits Dr, Bay City, MI 48706 U.S.A.

²Stony Brook University, 100 Nicolls Road, Stony Brook, NY 11794 U.S.A.

^agil.chung@sksiltron.com, ^brobert.viveros@sksiltron.com, ^ccharles.lee@sksiltron.com,

^dandrey.soukhojak@sksiltron.com, ^evladimir.pushkarev@sksiltron.com,

^fqianyu.cheng@stonybrook.edu, ^gbalaji.raghothamachar@stonybrook.edu,

^hmichael.dudley@stonybrook.edu

Keywords: 4H-SiC, X-ray topography, laser scanning, photoluminescence, basal plane slip band, bar stacking fault

Abstract. Correlation of X-ray topography and production line defect inspection tools has demonstrated the capability of in-line tools to differentiate between geometrically comparable basal plane slip bands (BPSB) and bar stacking faults (BSF) on 4H SiC wafers. BPSBs were found to propagate through epitaxial growth at high rates and with similar photoluminescence signatures to post-epitaxy BSFs. Molten KOH etching post-epitaxy provided evidence of distinguishing features between BPSBs and BSFs, suggesting that the defects were indeed correctly identified by in-line defect inspection tools pre-epitaxy.

Introduction

Accurate characterization of crystalline defects in 4H SiC is critical for advancing fundamental understanding of crystal growth, improving process controls, and enabling successful industrial applications. Among several applications, 4H SiC has attracted particular interest for power electronics because of intrinsic advantages such as higher temperature operation and reduced switching losses compared to conventional silicon-based devices [1]. On the other hand, limited process control over the densities of various crystalline defects in SiC, including basal plane dislocations (BPDs) [2, 3] and bar stacking faults (BSFs) [4], can significantly impact device yields. Synchrotron X-ray topography (XRT) has been applied for highly sensitive characterization of crystalline defects in PVT-grown SiC [5]. This technique has enabled the observation of basal plane slip bands (BPSBs), which are densely clustered arrays of parallel BPDs [6]. BPSBs present geometrically similarly to bar stacking faults (BSFs) on SiC wafers but are distinct defects. Herein, we report on production line metrology tool capability to detect and classify BPSBs as distinct defects from BSFs on test grade wafers as well as an investigation of defectivity propagation through epitaxial growth.

Experimental

4H n-type SiC boules were grown by seeded sublimation, and wafers were manufactured from boules using standard wafering and polishing processes. Wafers were imaged using synchrotron X-ray topography (XRT) and laser scanning (KLA Candela 8520) techniques. Monochromatic grazing incidence topography with $\vec{g} = 11\bar{2}8$ was used for XRT imaging. Candela 8520 scattered light and photoluminescence (PL) channels were used for BPSB and BSF detection, respectively. 14 μm thick epitaxy with $8.5 \times 10^{15} \text{ cm}^{-3}$ doping concentration was grown on Wafers 1, 3, and 4, and 6 μm thick epitaxy with $1.8 \times 10^{16} \text{ cm}^{-3}$ doping concentration was grown on Wafer 2. After epitaxial growth, wafers were scanned on Candela 8520 with modified scan and analysis conditions. Evaluation of

propagation through epitaxy was performed by correlating die occupancy of bare wafer BPSB and epi wafer defects. Lastly, molten KOH etching was performed on the wafers followed by imaging with confocal differential interference contrast (DIC) microscopy (Lasertec SICA88).

Results and Discussion

BPSB Observation with BSF-like Geometry. Prior studies have demonstrated that BSFs are formed by terrace nucleation as another polytype or by deflection of threading dislocations [4]. In contrast, BPSBs are formed by thermal stress and Frank-Read sources in the basal plane [6]. The BPSBs exist in the boule after growth, and segments of those BPSBs are contained within a wafer post-slice. Grazing incidence XRT has low penetration depth in a wafer, and consequently, BPSBs demonstrate BSF-like geometry (Fig. 1) despite their distinct etiologies.

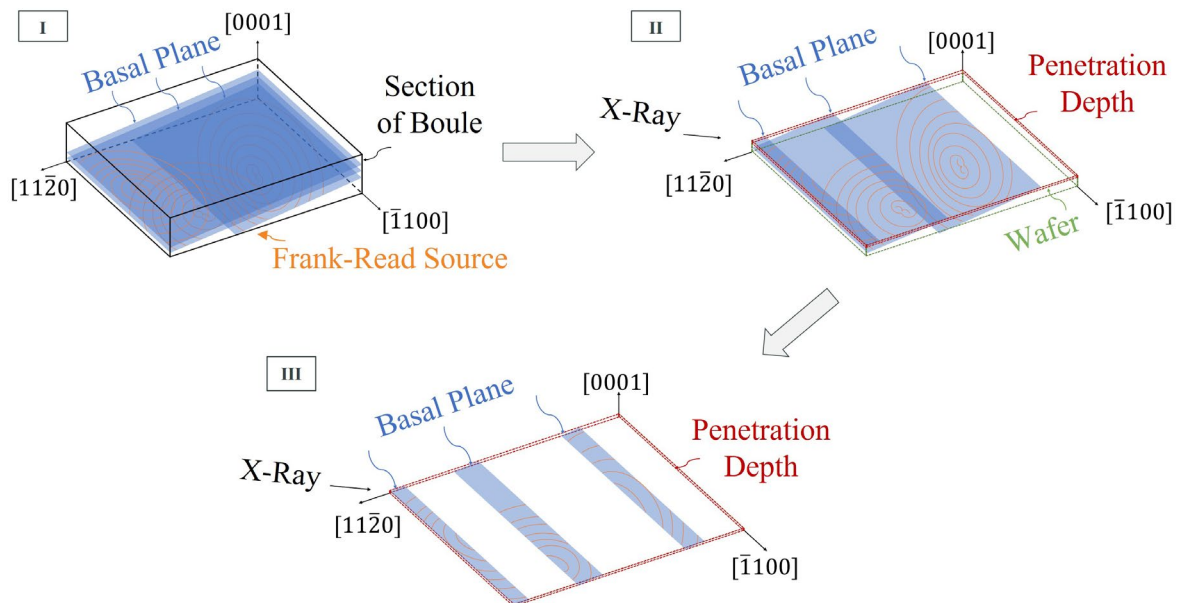


Fig. 1. Schematic of 3 BPSBs within SiC boule (I) and how they are visualized with BSF-like geometries in a single wafer (II) with XRT imaging (III).

BPSB Detection by X-Ray Topography and Laser Scanning. Synchrotron XRT was used to image putative BPSBs, which appear as BSF-like features but are composed of parallel BPDs that terminate at roughly the same edges (Fig. 2A). Laser scatter imaging of BPSBs demonstrated contrast against the crystal background (Fig. 2B) with minimal to no visible light (VIS) PL (Fig. 2C). Higher magnification XRT images from another wafer (Fig. 2D, E) highlight the generalized alignment of BPDs within these BPSBs.

In general, BPSBs were uniquely visible on the laser light scatter channel of the production line defect inspection tool (Fig. 3). In contrast, BSFs were detectable on the inspection tool according to their signatures on the VIS-PL channel.

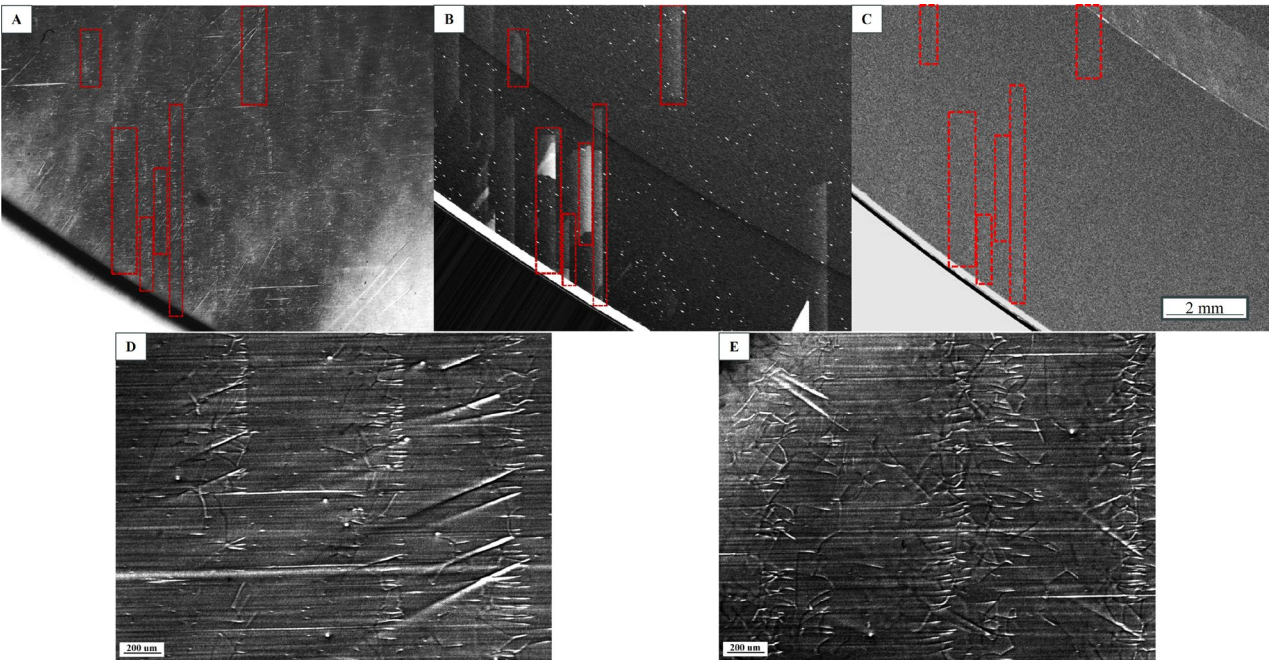


Fig. 2. Synchrotron XRT (A), light scattering (B), and VIS PL (C) images of BPSBs from the same wafer region. Higher magnification images of BPSBs as observed on XRT (D, E).

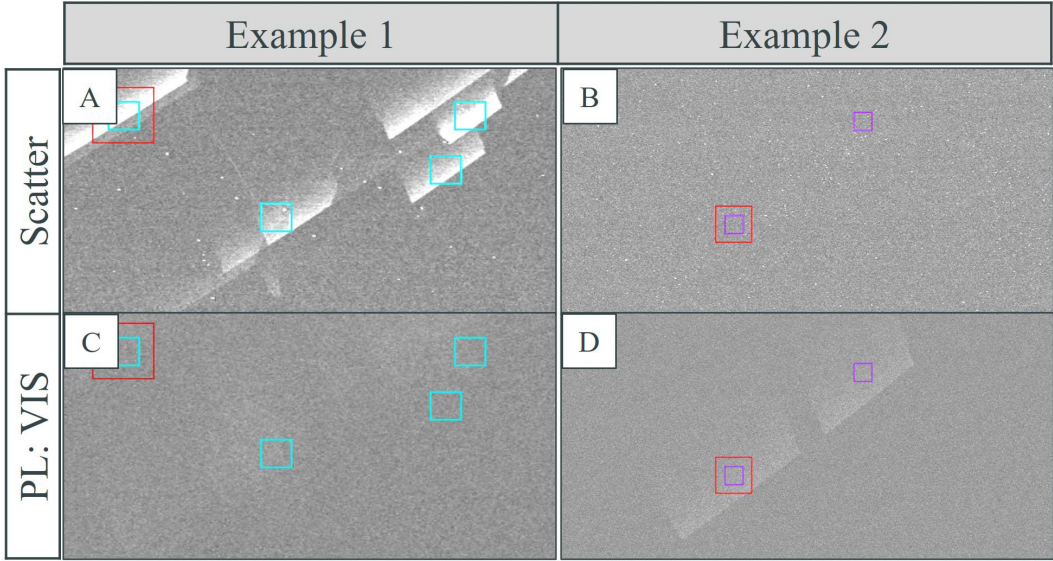


Fig. 3. Candela 8520 scatter (A, B) and PL (C, D) Mercator projection images. BPSBs demonstrate scatter contrast without PL contrast (A, C), whereas BSFs demonstrate PL. contrast (B, D). Field-of-view in each panel is 8 mm x 3.6 mm.

BPSB Propagation through Epitaxial Growth. SiC epitaxy was grown on wafers with BSFs and BPSBs as identified by laser scanning. BSF-like VIS and near ultraviolet (NUV) PL signatures were found where suspected BPSBs were observed prior to epitaxial growth. (Fig. 4A). Spatial correlation of bare BPSB and epitaxy BSF-like defectivity indicated roughly complete propagation of BPSBs through epitaxy (Fig. 4B), where incomplete propagation is hypothesized to primarily be a consequence of analytical methodology. Defect size is often

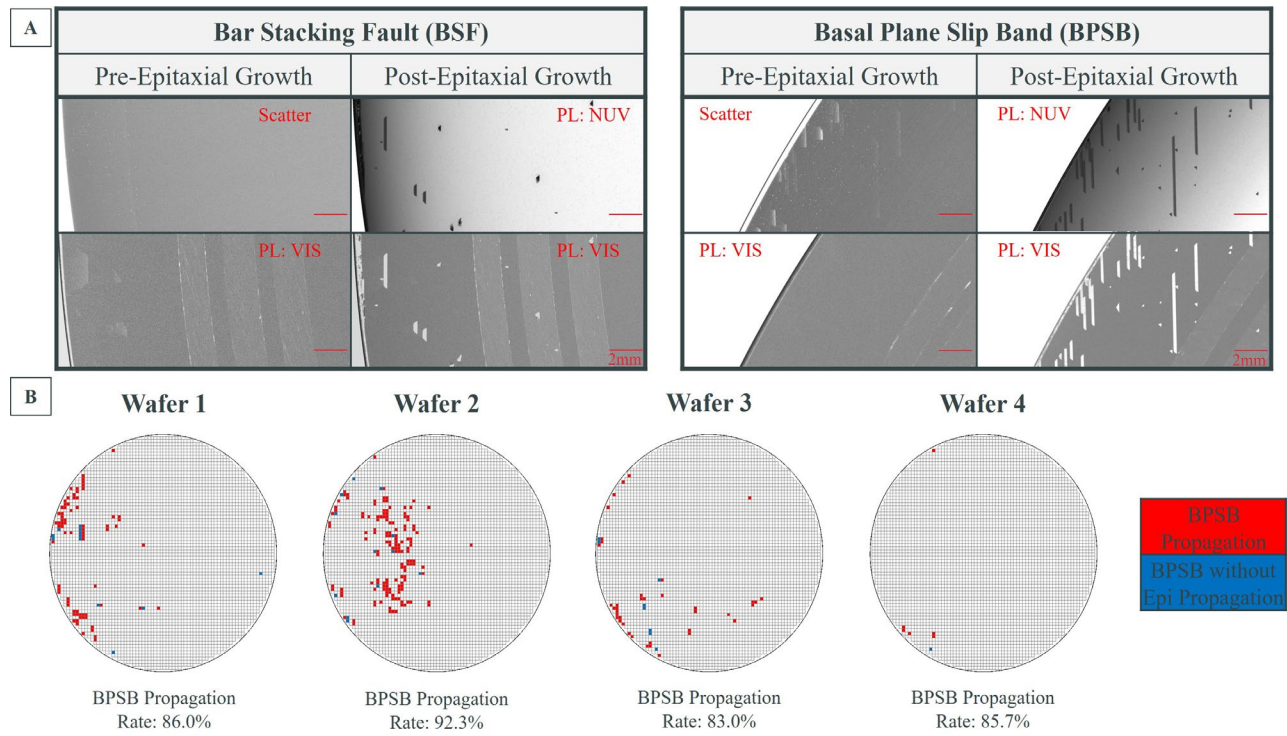


Fig. 4. Candela 8520 images of BSFs and BPSBs pre- and post-epitaxy (A). The defects demonstrate distinct signatures pre-epitaxy but comparable PL signatures post-epitaxy. Spatial correlation of detected BPSBs pre-epitaxy and PL signature post-epitaxy (B).

overestimated on bare wafer due to subsurface signal collection (Fig. 4B, Wafer 1 adjacent blue and red vertical lines), propagation estimation is subject to coordinate accuracy across two scans, and imperfections in defect detection/classification may further contribute to errors in this analysis. Similar post-epitaxy propagation of BSF and BPSB from bare wafer was an unexpected result and requires further investigation.

Evaluation of Dislocations by KOH Etching Post-Epitaxial Growth. As a first step to better understand the above result, the wafers were etched with KOH post-epitaxial growth and imaged using confocal DIC. Identified examples of BSFs demonstrated typical vertical step heights (Fig. 5A). On the other hand, suspected BPSBs demonstrated vertical alignment of threading edge dislocations (TEDs) or unconverted BPDs without the visible step height (Fig. 5B), indicating that the production line inspection tool correctly identified the two types of defects as distinct classes pre-epitaxial growth. BSFs with both PL and scattered light signatures were observed, however, highlighting potential future challenges in reliable separation across all process variation.

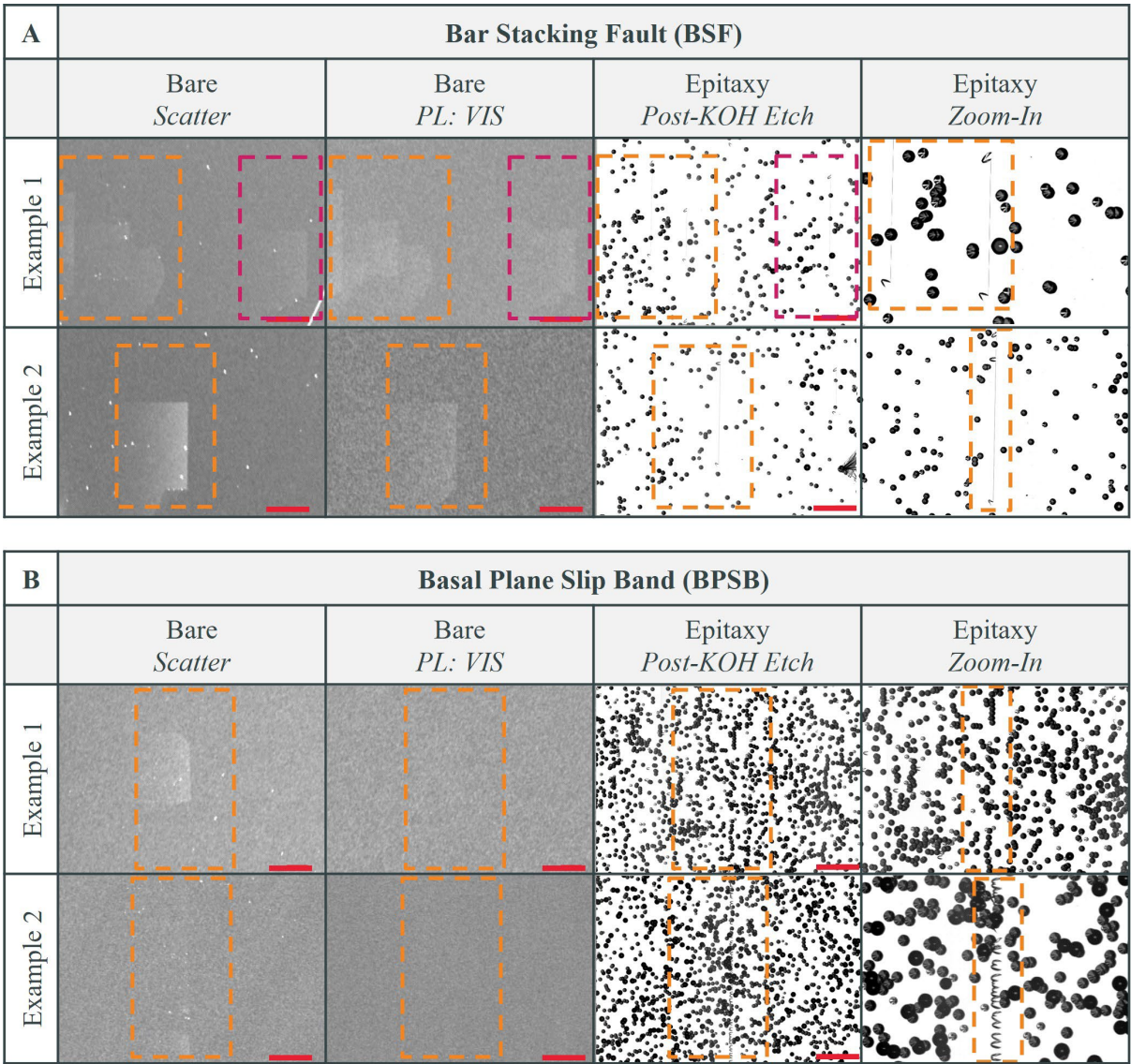


Fig. 5. BSF images by Candela 8520 scatter and PL pre-epitaxy and by SICA88 DIC of KOH etch post-epitaxy (A). BPSB images by Candela 8520 scatter and PL pre-epitaxy and by SICA88 DIC of KOH etch post-epitaxy (B). Dashed boxes outline the same regions across each image. Scale bar = 400 μm .

Summary

Production line defect inspection tools are capable of detecting BPSBs and differentiating such defects from BSFs pre-epitaxial growth. Further investigation of tool and/or analytical optimizations may improve classification purity and accuracy. BPSBs appear to propagate through epitaxial growth as BSF-like defects. Potential distinctions in KOH etch dislocation patterns, however, were observed between putative BSFs and BPSBs. Further investigation with XRT, particularly on wafers post-epitaxial growth, is necessary to better understand these observations.

References

- [1] X. She, A.Q. Huang, O. Lucia, B. Ozpineci, Review of silicon carbide power devices and their applications, *IEEE Trans. Ind. Electron.* 64.10 (2017) 8193-8205.
- [2] T. Kimoto, Material science and device physics in SiC technology for high-voltage power devices, *Jpn. J. Appl. Phys.* 54.4 (2015) 040103.
- [3] T. Ailihumaer, H. Peng, B. Raghothamachar, M. Dudley, G. Chung, I. Manning, E. Sanchez, Relationship between basal plane dislocation distribution and local basal plane bending in PVT-grown 4H-SiC crystals, *J. Electron. Mater.* 49.6 (2020) 3455-3464.
- [4] Y. Yang, J.Q. Guo, O. Goue, B. Raghothamachar, M. Dudley, G. Chung, E. Sanchez, J. Quast, I. Manning, D. Hansen, Synchrotron X-ray topography analysis of double Shockley stacking faults in 4H-SiC wafers, *Materials Science Forum*. Vol. 858. Trans Tech Publications Ltd (2016) 105-108.
- [5] B. Raghothamachar, M. Dudley, Dislocations in 4H-SiC substrates and epilayers, in *Wide Bandgap Semiconductors for Power Electronics: Materials, Devices, Applications*, Vol. 1, ch7, Wiley-VCH GmbH, Berlin, 2021.
- [6] S. Ha, M. Skowronski, W. Vetter, M. Dudley, Basal plane slip and formation of mixed-tilt boundaries in sublimation-grown hexagonal polytype silicon carbide single crystals, *J. Appl. Phys.* 92.2 (2002): 778-785.